Energy Conversion and Management 291 (2023) 117322

Contents lists available at ScienceDirect

Energy Conversion and Management

journal homepage: www.elsevier.com/locate/enconman

Syngas methanation over a metal hydride catalyst: Technology performance, efficiency and economic profitability

Nerijus Striūgas *, Kęstutis Zakarauskas, Rolandas Paulauskas, Aurimas Lisauskas, Adolfas Jančauskas

Laboratory of Combustion Processes, Lithuanian Energy Institute, Breslaujos str. 3, LT-44403 Kaunas, Lithuania

ARTICLE INFO

Keywords:
Syngas
Hydrogenation
Methane
Gasification
Metal hydride
Catalyst

ABSTRACT

In the last decade, biomass has been considered one of the main renewable energy sources to replace fossil fuels and consequently, biomass conversion technologies for the production of alternative fuels will play a specific role in the future energy as green biofuels for the transport sector or a power generation at small-scale distributed plants. During the thermal conversion - gasification, biomass is converted into more valuable products - syngases which could be used for biomethane production. Though, some challenges still exist related to the broad applicability of the thermal conversion of biomass to biomethane: costly short-life catalysts and a low conversion efficiency due to the high amount of carbon monoxide/dioxide in syngas.

To overcome these challenges, an innovative biomethane production concept based on the plasma-assisted gasification and conversion of synthetic gases to biomethane was developed and tested, including research on the adaptability of two catalysts, magnesium nickel and magnesium nickel hydride, for raw syngas conversion. The performance of catalysts was investigated in a fixed bed type reactor using raw syngas obtained from plasma-assisted gasification.

The results indicate the magnesium nickel hydride catalysts' good activity and functionality for converting carbon dioxide and carbon monoxide-containing syngas. A high conversion of 0.997 is reached. Determined that the surplus of hydrogen promotes the conversion of carbon oxides, though the volumetric concentration of methane (the maximum of 86.4 vol%) in product gas is reduced. Considering that the developed technology concept can be integrated into small combined heat and power plants, bio-waste generating plants, or decentralized areas as an additional source of renewable energy or biofuel production, the energy-mass balance and economic analysis for the optimization of 1 MWh bio-CH_4 production concept was provided.

1. Introduction

To achieve the Green Deal targets, the share of renewable energy sources (RES) in the final energy consumption should be increased, and fossil fuels substituted with low/zero carbon ones such as syngas, biomethane, hydrogen and ammonia (NH_3)). Biomass is considered one of the main renewable sources to replace fossil fuels. Consequently, biomass conversion technologies for the production of alternative fuels like biogas, biomethane, and syngas are gaining more attention [1]. During the thermal conversion - gasification, biomass is converted into more valuable products - syngases which could be used for direct combustion producing heat and electricity or for methanation. Besides, it is considered that the thermochemical conversion of the lignocellulosic biomass and undegradable waste will play a specific role in the future energy as a production source of green biofuels for the transport sector [2] or a power generation at small-scale distributed plants [3].

However, some challenges still exist related to biomass's thermal conversion to biomethane. To achieve the highest conversion rates of syngas to biomethane, the syngas mixture should consist only of H_2, CO_2 or/and CO (carbon monoxide), and the stoichiometric coefficients of the reactants in the hydrogenation process should be equal to 3 and 4, respectively [4]. However, the ratios of H_2:CO/CO_2 in the syngas from the woody biomass are lower, and the syngas composition depends on the gasifier type, gasification conditions, feedstock, temperature, or oxidiser [5].

To increase the quality of syngas in terms of the ratios of H_2:CO/CO_2, other technologies like electrolysis [6] or a plasma application [7] could be used onsite. In the case of electrolysis, a smaller amount of green

* Corresponding author.
E-mail address: Nerijus.Striugas@lei.lt (N. Striūgas).

https://doi.org/10.1016/j.enconman.2023.117322

Available online 20 June 2023

hydrogen could be introduced into the syngas stream to reach stoichiometric coefficients of the reactants in the methanation process resulting in higher efficiency and methane yield [8]. Meanwhile, the plasma has broader applicability. During the gasification, the obtained syngas could be treated by thermal plasma to completely crack tars, reform organic sulphur compounds and increase concentrations of H_2 [9]. Also another option is to convert various wastes to more valuable gases and direct them to the syngas stream from the gasifier to enhance the composition of syngas. For example, waste glycerol conversion by a microwave plasma results in gases consisting of H_2, CO and CH_4 [10]. Another research [11] shows that using the thermal plasma, the waste glycerol is converted mainly to H_2 and CO with concentrations of 57.87 vol% and 21 vol%, respectively.

Another challenge related to biomethane production from raw syngas is the need for low-cost, long-term and high-activity catalysts, which are still in the research and development stage. For example, nickel catalysts doped on various substrates are gaining much attention as cost-effective catalysts [12]. Still, a carbon deposition leading to the lower conversion efficiency of syngas should be solved [13]. One of the recent works [14] demonstrates that the vanadium (V) promoting of Ni/Al_2O_3 catalyst causes structure changes resulting in a low-temperature activity increase. At the same time, the use of bimetallic composites improves some of the catalyst properties. Meanwhile, adding magnesium (Mg) enhances the catalytic activity regarding chemisorption and dissociation of CO_2 and improves the oxidative environment around the Ni particles in the catalyst [15]. Li et al. [16] investigated the effect of the Ni/Mg ratio in the structured catalysts on CO_2 conversion and CH_4. The Ni/Mg ratio of 4 to 1 led to higher catalytic activity and stability over a long work (100 h) at a pretty low operation temperature of 300 °C with 87% conversion of CO_2.

This synergistic effect between metals prevents the agglomeration of Ni active centres [17] and ensures an ability to avoid CO poisoning and resistance against coke formation [18] while maintaining a very high conversion efficiency [19]. The $NiMg/Al_2O_3$ catalyst showed a stable syngas methanation process in a fluidised bed. The selectivity of CH_4 was 77%, but $CO:CO_2$ ratio should be controlled to prevent suppression of the water gas shift and Boudouard reactions [20]. Wang et al. [21] investigated three types of specially prepared nickel–magnesia solid solution catalysts (Ni/Mg, Ni/MgO and $Ni_{0.03}/Mg_{0.97}O$) for tar reforming in a fluidised bed and syngas conversion to methane. Ni/MgO catalysts demonstrated better catalytic activity under lower temperatures but a lower carbon conversion to methane (~77%). Meanwhile, NiO/MgO showed better reforming performance stability under higher temperatures and a conversion efficiency of 79.9%. Another research [22] tested 20 wt% NiO and 2 wt% MgO catalysts for methanation under the dual fluidised bed (DFB) conditions and additionally introduced the sorption enhanced reforming (SER). According to [22], the SER improves the H_2:COx ratio, and methanation efficiency increases from 73% to 95%. Also, a catalyst of Mg_2NiH_4 was tested for CO_2 hydrogenation to methane [23]. It was found that the catalyst remains still efficient after many hydrogen sorption cycles during CO_2 and CO hydrogenation and achieves a CO_2 conversion of 0.67. Though, its performance for raw syngas conversion to methane has not been studied.

Overall, to integrate the syngas methanation technology into small combined heat and power plants, bio-waste generating plants, or decentralized areas, the sufficient syngas composition and the low cost, stable and high activity catalyst are still crucial factors in the methanation of the raw syngas to obtain high conversion and high methane selectivity. Therefore, the present work demonstrates a bio-CH_4 production concept based on plasma-assisted gasification and conversion of synthetic gases to biomethane using a new metal hydride catalyst. To explore the performance of the catalyst for the methanation process of raw syngas and perform optimization of operating conditions, the catalyst was tested in a fixed bed type reactor using syngas obtained from wood chips gasification by changing gas hourly space velocities, reactor temperature, H_2:COx ratio, and the Ni concentration in the catalyst bed. Considering that the developed concept of technology can be integrated into existing systems, the energy-mass balance and economic analysis for the optimization of the 1 MWh bio-CH_4 production concept was provided.

2. Materials and methods

This section provides a general overview of the methods used for the research. It consists of a detailed description of materials used for catalysts and their synthesis method, the production of raw synthesis gases using plasma-assisted gasification, and their conversion to biomethane in the context of the problem to be analysed. Also, an explanation for estimating the proposed technology's economic evaluation is included.

2.1. Catalyst preparation and analysis

Two different metal alloys as catalysts (Mg_2Ni and Mg_2NiH_4) were prepared for the experiments.The Mg_2Ni powder was produced by milling original alloy pellets with an average diameter of 3 mm and Mg_2Ni purity of 99% (American elements).The Mg_2Ni alloy pellets were mechanically ground down to a grain size of 20–50 μm. Part of these powders has been set aside for further hydrogenation tests, while the rest were used for further synthesis of Mg_2NiH_4. For this reason, the Mg_2Ni powder was placed into a stainless-steel reactor for several hours in a vacuum. After this, activation of the Mg_2Ni powders was started by applying 4 hydriding (16 h at 250 °C under 20 bar H_2) and dehydriding cycles (8 h at 250 °C in a vacuum). The final hydriding was applied for 24 h at 250 °C under 20 bars of H_2 before the methanation. A more detailed discussion on catalyst analysis can be found in previous work [24].

In [17], the authors report that the catalyst can achieve the best activity and low CO yield at a Ni concentration of 20 wt%. It is also mentioned that above this Ni concentration, thermal agglomeration occurs, which leads to the destruction of the catalyst structure. For this reason, the upper concentration of Ni in the catalyst bed was taken to be 20 wt%. In addition, a lower loading value of 10 wt% was chosen to compare the influence of the Ni content on the catalyst performance. To get the desired amount of Ni in the catalyst, the Mg_2Ni or Mg_2NiH_4 was mixed with the Al_2O_3 powder, and approximately 8.8 g was placed in the central part of the reactor (Fig. 2). This is done to increase the reaction volume and avoid the agglomeration of active particulates caused by the hot spot.

2.2. Syngas production facility for methanation

The raw syngas was obtained from a plasma-assisted gasification system consisting of a downdraft gasifier for solid biofuel conversion and a plasma chemical reactor for liquid biofuel conversion. The plasma gasification system consists of 5 main parts: a solid biofuel feeding system, a downdraft gasifier, a gas cleaning system, a plasma chemical reactor and a combustion chamber with a gas burner (Fig. 1). More detail on the downdraft gasifier and plasma chemical reactor are presented in these works [11,25]. Syngas was produced by a gasifying mix of wood chips from a local supplier under an oxygen environment. The obtained syngas in the gasifier was directed to the plasma chemical reactor, where supplied syngas partially decomposed, and the complete conversion of additional bio-oil (waste glycerol) in the steam environment was performed.

The simultaneous use of several fuels allows the ratio of the main syngas products, H_2/CO and H_2/CO_2, to be increased and controlled.. For downdraft gasification only, the H_2/CO and H_2/CO_2 ratios for solid biomass gasification are approximately 0.71 and 1.85, respectively.. In contrast, these ratios for converting of liquid biofuels in a plasma chemical reactor in a steam environment are 2.74 and 3.19, respectively. When the two systems are combined, part of the CO coming from the downdraft reactor reacts with H_2O in the plasma reactor to produce

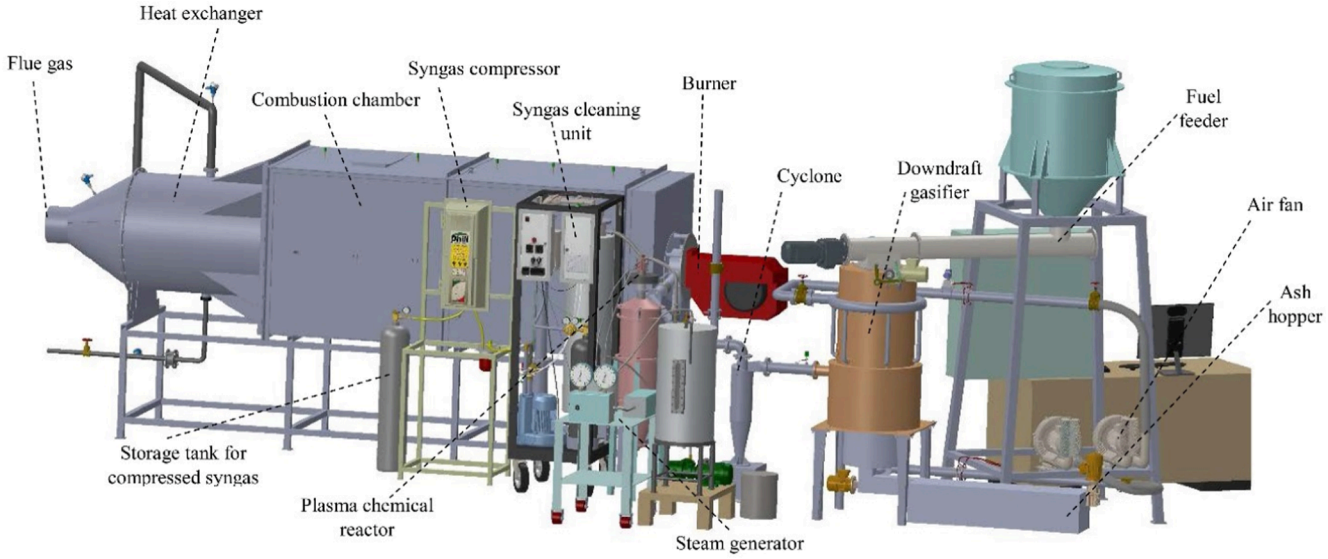

Fig. 1. Plasma-assisted gasification unit for hydrogen rich syngas production.

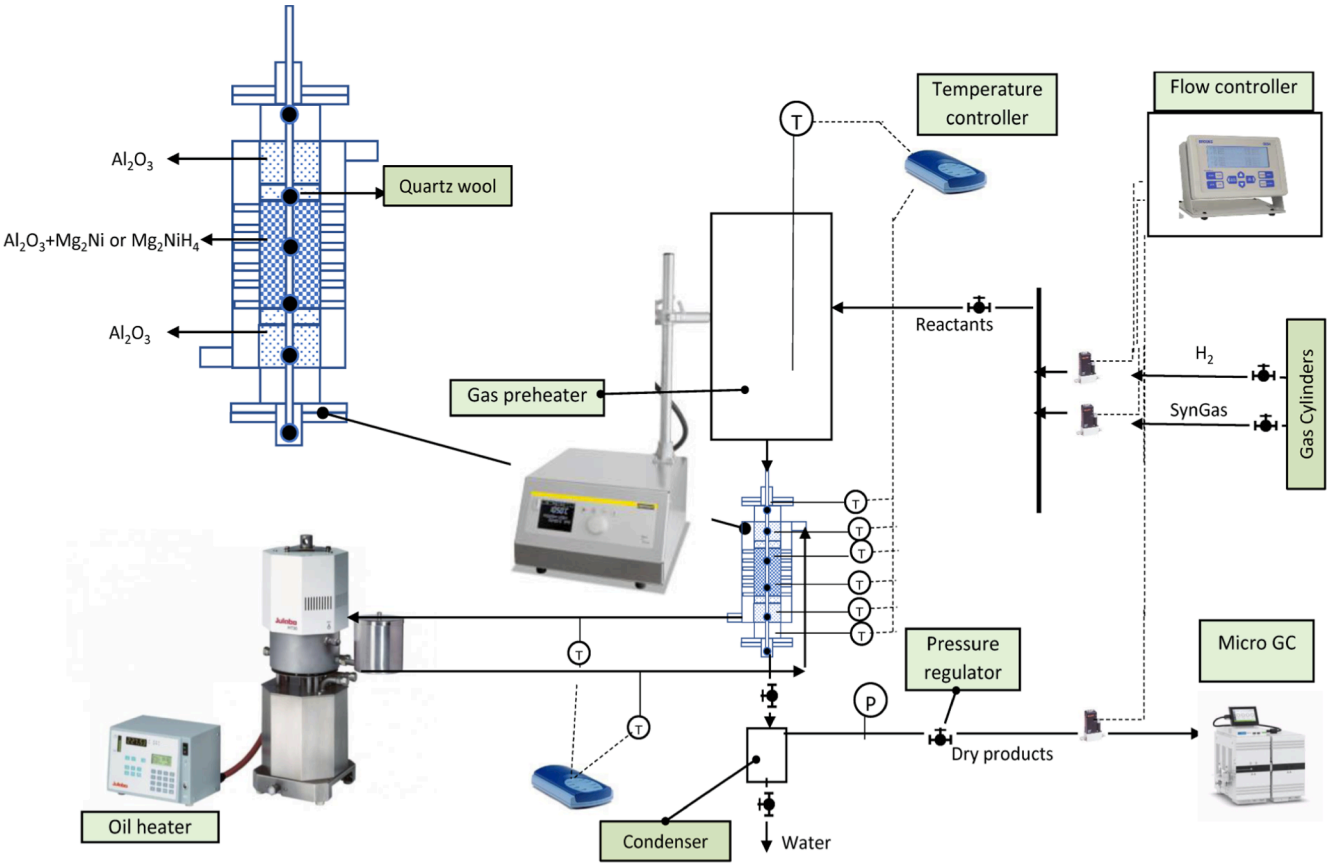

Fig. 2. Scheme of the COx hydrogenation setup.

additional H_2 and CO_2, resulting in a total H_2/CO and H_2/CO_2 ratio of 1.21 and 2.46 respectively. The upgraded syngas is fed into a gas cleaning system. A high-temperature (550 °C) cyclone is first used to remove the particulates. The gas then passes through a high-temperature (450 °C) ceramic filter, which further breaks down the tar compounds and removes the remaining fine particulates. Finally, a tubular condenser is used to remove any remaining condensable tar compounds and water. The clean and dry gas that comes out is directed to a Phill HRA-P30 gas compression unit.Syngas is compressed up to 100 bar using the compression unit and stored in gas cylinders, which are further used in the methanation facility. The composition of obtained syngas is presented in Table 1.

2.3. Syngas methanation setup

The experimental setup for syngas COx hydrogenation consists of a

Table 1
The syngas composition obtained from the plasma-assisted gasification system.

Parameter	Value
Syngas composition, vol%	
H_2	47.61
CO	27.13
CO_2	18.73
CH_4	4.05
C_2H_2	0.24
C_2H_6	0.24
C_3H_8	0.04
O_2	0.52
N_2	1.16
Syngas specific ratios:	
H_2/CO	1.75
H_2/CO_2	2.54
$H_2/(CO + CO_2)$	1.03

methanation reactor with a hot-oil heating/cooling system, a gas mixing system, a reaction product cooler, and a semi-online gas analyser Agilent Micro GC990 (Fig. 2).

The raw synthetic gas from the cylinder was fed into the gas mixing system of the methanation reactor (Fig. 2). Knowing that the ratio of the main syngas components H_2:COx is less than the required ratio according to the stoichiometric reaction equations ($CO + 3H_2 \leftrightarrow CH_4 + H_2O$) and ($CO_2 + 4H_2 \leftrightarrow CH_4 + 2H_2O$), the addition of pure hydrogen is added from the gas cylinder.

The prepared mixture is fed into the gas heater where the gas mixture is preheated to a temperature of approximately 300 °C and then directed to the methanation reactor. In the methanation reactor, the prepared catalyst was placed between two layers of Al_2O_3 (2 g each) and quartz wool. The hydrogenation of COx in the syngas was analyzed using two different concentrations of Ni − 10 wt% and 20 wt%.

The reactor temperature profile over the height was determined using a multi-point thermocouple installed in the centre part of the reactor. At least three thermocouple parts were in contact with the active bed layer. To initiate the reaction, thermal oil with a preset temperature of 300–360 °C is supplied from the oil heater. The thermal oil is also used as a coolant to maintain a stable bed temperature and avoid hot spots, as the highly exothermic methanation reaction generates a lot of heat [26], especially in the initial part of the catalyst. After the reaction, the gas enters a water-cooled condenser, where the water vapour generated in the reaction condenses. Additionally, a gas pressure regulator is installed behind the condenser to maintain a constant reaction pressure of 10 bar to increase the process efficiency. Finally, the reaction products are fed to a semi-online gas analysis system, the Agilent Micro GC 990. The main parameters of methanation are presented in Table 2.

The different gas hourly space velocities (GHSV) were applied to test the performance of flow loads on the catalyst bed, which calculated as follows:

$$GHSV = Q/V \tag{1}$$

where GHSV – space-velocity, h^{-1}; Q – flow of reactant through the catalyst bed, m^3/h; V – volume of catalyst in the bed, m^3.

Table 2
Main parameters of syngas methanation.

Parameter	Value
Catalyst:	10 wt% and 20 wt% of Ni
Mg_2NiH_4 in Al_2O_3	
Mg_2Ni in Al_2O_3	
H_2:COx	1 and 1.2
Pressure	10 bar
Thermal oil temperature	300–360 °C
Reactant flow GHSV	6000–28000 h^{-1}

To evaluate the process performance are used two main parameters: the conversion of CO + CO_2 (X_{COx}) in syngas and the methane concentration in dry products gas (Y_{CH4}, vol%). The X_{COx} was calculated as follow:

$$X_{CO_x} = \frac{\left(V_{CO+CO_{2,in}} - V_{CO+CO_{2,out}}\right)}{V_{CO+CO_{2,in}}} \tag{2}$$

where $V_{(CO+CO2)}$ are the volumetric flow in l/min of CO and CO_2 at the inlet (in) and outlet (out) of the reactor.

The methane selectivity S_{CH4} was calculated as follows:

$$S_{CH_4} = \frac{Y_{CH_4}}{X_{CO_x}} \tag{3}$$

The values of the gaseous product concentrations after gasification and compression in the gas cylinder are obtained by averaging the results of at least three measurements with an overall uncertainty of up to 10 %. Meanwhile, before the methanation reactor (where the gaseous products are mixed with additional hydrogen gas) and after the methanation reaction (where the reaction product water is condensed), the composition of the gaseous products is measured with a semi-continuously running gas analyser providing results every 2 to 3 min. The examined values are obtained by averaging the values of five measurements with up to 10% overall uncertainty.

2.4. Economical analysis of bio-methane production concept

A detailed cost estimation of syngas-to-biomethane concept development was conducted based on two investment pathways: 1) the equipment-only investment (bioCH_4-case1) and 2) the greenfield investment (bioCH_4-case2). The levelised cost of synthetic natural gas ($LCOCH_4$), net present value (NPV), and payback period assessment of investment costs (CAPEX) were made according to equipment costs for the gasification based biofuel production system producing SNG [27] and based on investment costs of the "GoBiGas" bio-methane plant [28], which was already in operation. The required investments for the individual technological units and techno-economic data were recalculated for the bio-methane production of 1 MW (see Table 3). Below are presented equations for investment calculation:

$$LCOCH_4 = \frac{C_t}{\mathrm{HLH} \times P} \tag{4}$$

where P is the production capacity, MW; HLH is hours worked per year; C_t is annual cost of production in € (5);

$$C_t = FCF \times C_i \times C_s + C_{input} + C_{O\&M} \tag{5}$$

where C_i is the investment cost (6), €; C_S is subsidy factor, %; C_{input} is the cost of fuel; $C_{O\&M}$ is operating and maintenance cost, €; FCF is the fixed charge factor (7);

$$C_i = C_{Inv,ref,i}\left(\frac{P}{P_{ref}}\right)^{SF_i} \tag{6}$$

where P_{ref} and $C_{Inv,ref,i}$ are the capacity and investment of equipment, SF_i – scaling factory for specific installation [28];

$$FCF = \frac{r \times (1+r)^n}{(1+r)^n - 1} \tag{7}$$

where n is the economic lifetime base year (n = 25 years), and r is the discount rate (Table 3).

3. Results

Developing new technologies or adapting new elements to existing ones, always strive to optimise the key process parameters that will

Table 3
Parameters and assumptions for economic analysis of 1 MWh bio-CH_4 production.

	Case of investment in equipment (bioCH_4-case1), €/MWh	Case of Greenfield investment (bioCH_4-case2), €/MWh
CAPEX		
Fuel handling system	680 249	680 249
Gasification and combustion	294 991	294 991
Plasma chemical reactor	113 130	113 130
Gas cleaning system	344 107	344 107
Tail gas system	140 340	140 340
Compressors	100 000	100 000
Electrolysis unit	63 296	63 296
Methanation unit	245 676	245 676
Gas drying	49 715	49 715
Auxiliary equipment	–	2 297 132
Buildings and infrastructure	–	3 259 092
Structural steel	–	874 142
Piping and mechanical equipment	–	2 133 781
Start-up	2 221 852	2 221 852
Total investments	4 253 356	12 817 503

	Case for high price	Case for medium price	Case for low price
Natural gas, €/MWh	250	150	50
Biomas, €/MWh	39	30	15
Electricity, €/MWh	230	90	30
OPEX			
Staff, €/MWh_{prod}	8.1	8.1	8.1
Maintenance, €/MWh_{prod}	1.31	1.31	1.31
Gasifier component, €/MWh_{prod}	15	15	15
Plasma chemical reactor component, €/MWh_{prod}	3.3	3.3	3.3
Electrolysis unit component, €/MWh_{prod}	0.44	0.44	0.44
Materials used			
Other, €/MWh_{prod}	0.79	0.79	0.79
Other expenditure, €/MWh_{prod}	390	390	390
Discount rate, %	20	12.5	5
Plant lifetime, year	25	25	25

allow the process to run optimally, with minimum material consumption, maximum yields, and energy- and cost-efficiently. This chapter summarises the study's main results, highlighting the optimal process parameters, energy efficiency, and economic attractiveness of the proposed technology process.

3.1. Syngas conversion using magnesium nickel and magnesium nickel hydride

This section provides results and insight into the COx containing syngas conversion and methane generation using two types of catalysts, namely Mg_2Ni-Al_2O_3 and Mg_2NiH_4-Al_2O_3. Performed experimental tests revealed that the highest conversion (X_{COx}) of 0.997 was found for hydride catalyst containing Ni of 20 wt%, running the reaction with a stoichiometric ratio of 1.2, keeping thermal oil temperature of 360 °C and a GHSV of 6300 h^{-1} (Fig. 3). Increasing the GHSV rate, the conversion decreased in all cases studied, showing the limit over which the conversion of COx gases is not completed. The attempt to vary the stoichiometric ratio of hydrogen to COx gas has revealed that slightly higher conversions are achieved in excess hydrogen and at higher Ni concentrations.

The X_{COx} also reduced with a reduction in the temperature of thermal oil (Fig. 4). This effect is more intense at the lower concentrations of the catalyst active element (Ni), especially in the case of a hydride catalyst. It was also found that in the case of the hydride catalyst with H_2:COx = 1 and a Ni concentration of 10 wt%, the temperature dependence of the X_{COx} was higher than in the case of the Ni_2Mg alloy.

The concentration of reaction products was measured during all runs of experiments and several times at each point to minimize the deviation between results. Figs. 5 and 6 show the volumetric concentration of methane, as the main constituent of the resulting gas mixture, in the dry gaseous product stream as a function of GHSV and catalytic reactor temperature. During the first run, when the stoichiometric ratio was adjusted to 1.0 at 360 °C, 10 wt% of Ni, and the lowest GHSV, the methane concentration was reached its maximum 83.8 vol% using Mg_2Ni as a catalyst. At the same conditions using Mg_2NiH_4, the maximum methane concentration was a bit higher 84.8 vol%. Further, methane concentration decreased with the increase in the GHSVs to almost 28000 h^{-1} (Fig. 5). At this point, as mentioned before, the conversion of carbon oxides reduces, thus reducing methane concentration as well. Therefore, the smallest CH_4 concentrations were obtained for both types of a catalyst having Ni of 10 wt% and, despite the different stoichiometric ratios, were in the very same range, 72.5 vol% @ H_2:COx = 1.2, 73.9 vol% @ 1.0 and 73.8 vol% @ 1.2; 73.6 vol% @ 1.0 respectively.

Further performance test on the methane synthesis changing the thermal oil temperature shows that CH_4 volumetric concentration

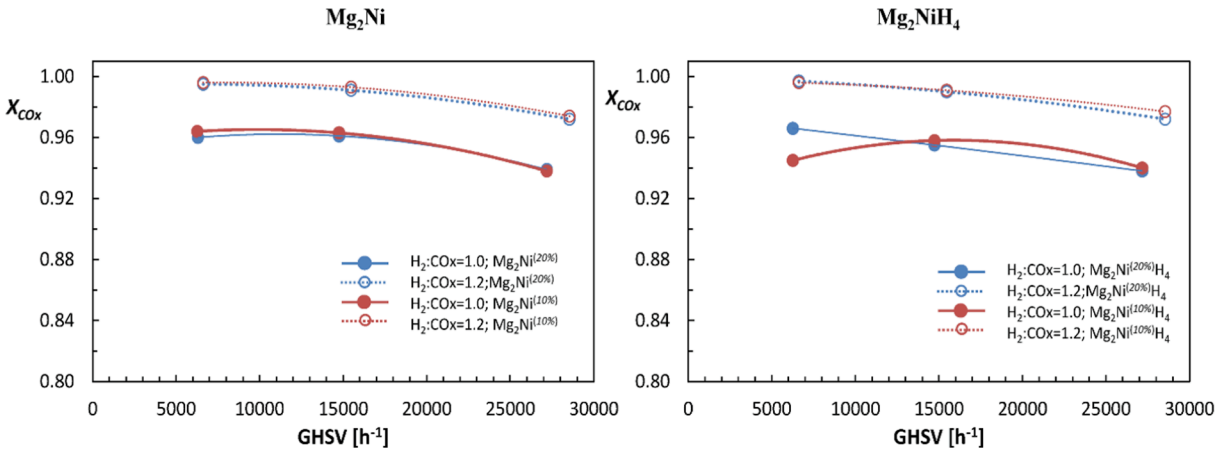

Fig. 3. COx gas conversion versus reactant gas hourly space velocity (GHSV) using Mg_2Ni and Mg_2NiH_4 catalyst containing different Ni amount of 10 wt% and 20 wt % at different H_2:COx ratios and constant T_{oil} = 360 °C.

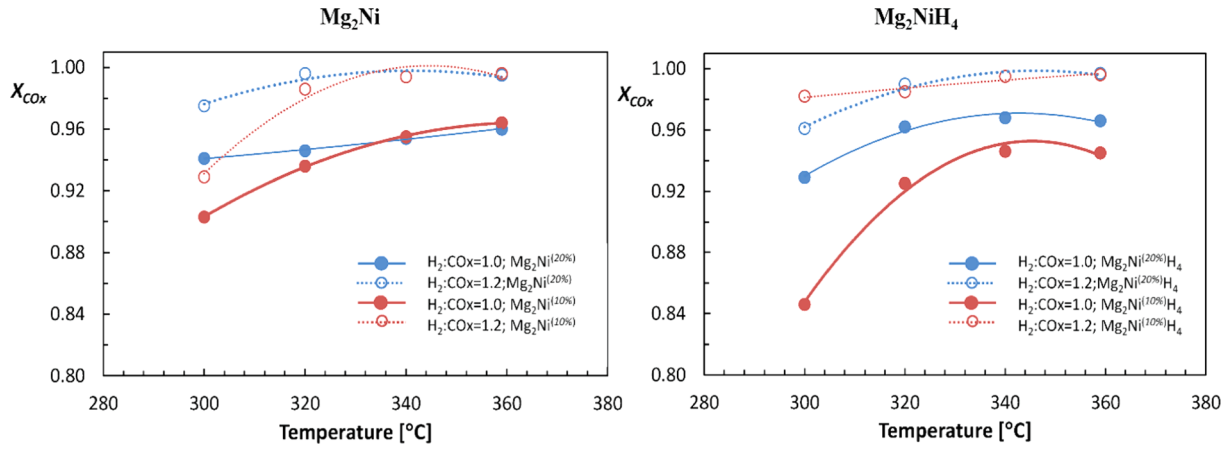

Fig. 4. COx gas conversion versus reactor temperature (T_{oil}) using Mg_2Ni and Mg_2NiH_4 catalyst containing different Ni amount of 10 wt% and 20 wt% at different H_2:COx ratios and constant GHSV = 6300 h^{-1}.

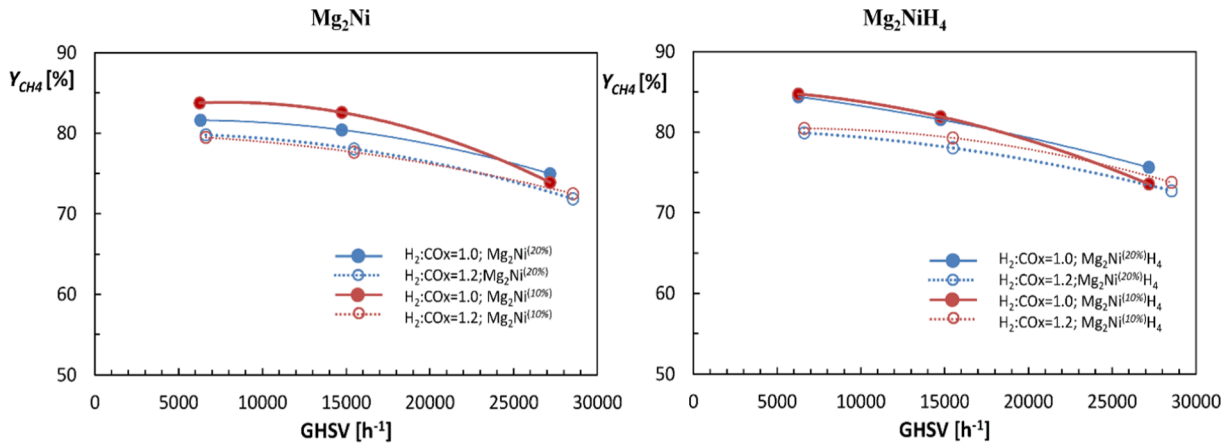

Fig. 5. Concentration of CH_4 in dry hydrogenation products versus GHSV using Mg_2Ni and Mg_2NiH_4 catalysts containing different Ni amount of 10 wt% and 20 wt% at different H_2:COx ratios and constant T_{oil} = 360 °C.

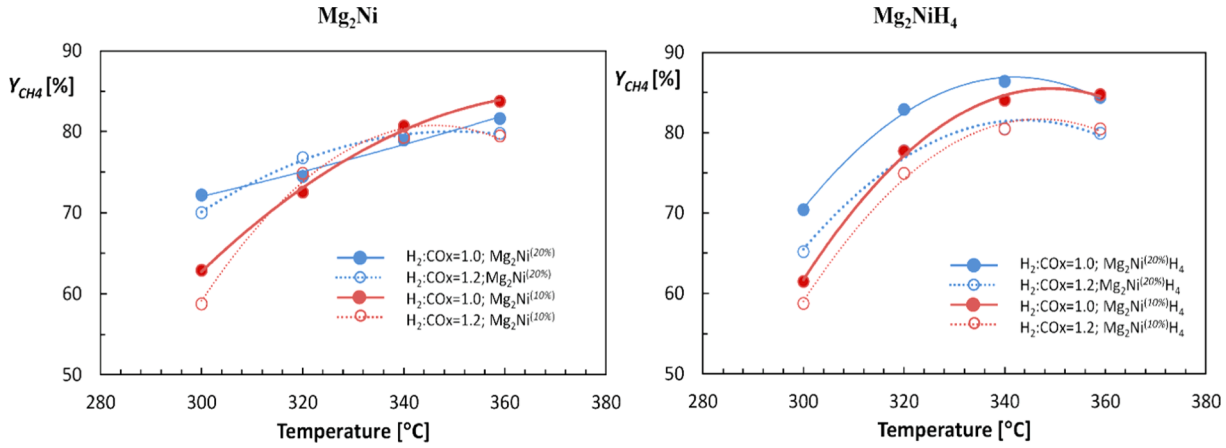

Fig. 6. Concentration of CH_4 in dry hydrogenation products versus reactor temperature (T_{oil}) using Mg_2Ni and Mg_2NiH_4 catalyst containing different Ni amount of 10 wt% and 20 wt% at different H_2:COx ratios and constant GHSV = 6300 h^{-1}.

correlate with COx conversion. The reduction of reactor temperature leads to an almost linear decrease in methane concentration using a Mg_2Ni catalyst. When the stoichiometric ratio was adjusted to 1.0, at the temperature of 360 °C, 10 wt% of Ni, and the lowest GHSV, the concentration reached 83.8 vol% for Mg_2Ni (Fig. 5). However, the situation in the case of Mg_2NiH_4 was slightly different. The highest methane concentration of 86.4 vol% was found at 340 °C working with hydrid containing 20 wt% of Ni and the lowest GHSV. For instance, considering the methane concentration at 360 °C, the difference is insignificant. It thus can be concludedthat this temperature range is optimum for maximum CH_4 concentration in gaseous products. When looking at the effect of the H_2:COx ratio on methane concentrations, no significant

difference was found, at least within the studied range. The excess hydrogen only reduced the volume concentration of methane in the product gas by a few percentage units. The influence of the Ni content in the catalyst bed also did not significantly affect on the change in concentration.

The other main products identified in the gas mixture were unreacted hydrogen and carbon dioxide (Table 4). Carbon monoxide was not detected, or if detected, at extremely low concentrations. CO completely converted due to its very high activity. This situation was observed in all tests.

The initial synthetic gas mixture always contained low concentrations of other light gaseous hydrocarbons. After the reaction, the volumetric concentrations of C_2H_6 and C_3H_8 varied only slightly and were of the same order of magnitude as in the initial gas mixture (Table 4). However, the situation for C_2H_2 gas was different since this compound was no longer detected in the products after the reaction.

3.2. Temperature profile in the methanation reactor

Figs. 7 and 8 present the temperature distribution over the height of the methanation reactor. Temperatures were measured during the hydrogenation of syngas containing carbon oxides over Mg_2Ni and Mg_2NiH_4 catalysts having different amounts of Ni, 10 wt% and 20 wt%. The first experimental trial maintained constant GHSV = 6300 h^{-1} stepwise changing the T_{oil} temperature from 300 to 360 °C and at H_2:CO_x ratios 1.0 and 1.2 (Fig. 7). As can be seen from the provided figure, changing the stoichiometric (H_2:CO_x) ratio in all cases studied had practically no effect on the temperature distribution in the reactor or in the catalyst bed and was the same for both ratios. The hot oil temperature fed to the reactor and the type of catalyst greatly impacted the reaction performance and, thus, the specific temperature distribution. In the first part of the reactor at T1, the reactants come from the preheater at a certain temperature. The hot oil circulating through the reactor is fed from the top and flows downwards. The starting temperature of the hot oil was 300 °C.

It was selected by performing a quick screening test to reveal the optimal temperature at which stable conversion of continuous reactants flow occurs. Therefore keeping this reactor temperature, the reactants reach the first contact with the catalyst, where the highly exothermic reaction starts immediately, and the temperature increases to some extent (Fig. 7). The released heat is then distributed downwards. In all cases, a peak temperature point was identified in the reactor, which is

Table 4
Composition of dry gaseous products after methanation reaction.

Catalyst	H_2:COx	GHSV, h^{-1}	Temperature, °C	Composition of dry gaseous products, vol%							S_{CH4}
				H_2	CO	CO_2	CH_4	N_2	C_2H_6	C_3H_8	
$Mg_2Ni^{(10\%)}$	1.0	6300	300	27.30	0.05	5.98	62.91	1.49	1.80	0.08	0.82
			320	19.52	0.02	4.51	72.54	1.63	1.35	0.05	0.83
			340	13.16	0.03	3.26	80.71	1.74	0.73	0.02	0.82
			360	11.38	0.01	2.72	83.76	1.73	0.03	0.01	0.82
		15,000	360	11.75	0.01	2.76	82.59	1.79	0.28	0.00	0.72
		28,000	360	18.25	0.02	4.26	73.88	1.74	0.24	0.05	0.59
	1.2	6300	300	32.65	0.05	4.16	58.77	2.22	1.69	0.08	0.84
			320	20.74	0.02	0.97	74.86	1.65	1.34	0.05	0.83
			340	17.51	0.02	0.40	79.28	1.67	0.66	0.09	0.82
			360	17.95	0.00	0.26	79.47	1.72	0.21	0.01	0.83
		15,000	360	19.01	0.00	0.46	77.65	1.69	0.25	0.06	0.72
		28,000	360	22.42	0.01	1.68	72.48	1.51	0.21	0.06	0.60
$Mg_2Ni^{(20\%)}$	1.0	6300	300	20.03	0.03	4.16	72.20	1.51	1.66	0.06	0.83
			320	18.74	0.06	3.82	74.49	1.61	0.92	0.03	0.83
			340	15.13	0.04	3.36	78.98	1.67	0.48	0.01	0.82
			360	12.74	0.01	2.96	81.62	2.04	0.23	0.03	0.82
		15,000	360	12.03	0.02	2.95	80.42	1.67	2.10	0.01	0.74
		28,000	360	17.40	0.05	4.15	74.96	1.63	0.23	0.00	0.61
	1.2	6300	300	24.86	0.07	1.56	70.00	1.49	1.63	0.06	0.83
			320	20.11	0.01	0.29	76.78	1.58	0.83	0.02	0.83
			340	18.12	0.05	0.33	79.30	1.58	0.26	0.02	0.82
			360	17.78	0.00	0.36	79.79	1.61	0.06	0.00	0.81
		15,000	360	18.70	0.00	0.62	78.06	1.56	0.17	0.00	0.72
		28,000	360	23.07	0.02	1.74	71.84	1.48	0.21	0.01	0.59
$Mg_2Ni^{(10\%)}H_4$	1.0	6300	300	28.35	0.07	6.25	64.49	1.57	1.82	0.09	0.82
			320	15.04	0.01	3.60	77.71	1.73	1.48	0.06	0.82
			340	10.26	0.01	2.78	84.05	1.73	0.78	0.02	0.83
			360	9.79	0.00	2.76	84.76	1.79	0.28	0.27	0.82
		15,000	360	12.13	0.02	3.16	81.93	1.72	0.22	0.00	0.72
		28,000	360	19.04	0.06	4.06	73.55	1.59	0.15	0.00	0.60
	1.2	6300	300	29.50	0.08	7.30	58.77	1.62	1.95	0.09	0.82
			320	20.51	0.04	1.19	74.93	1.52	1.41	0.06	0.82
			340	16.65	0.00	0.35	80.43	1.59	0.51	0.09	0.82
			360	16.99	0.01	0.30	80.46	1.56	0.30	0.00	0.82
		15,000	360	17.46	0.00	0.64	79.29	1.60	0.15	0.00	0.72
		28,000	360	21.43	0.01	1.51	73.76	1.54	0.13	0.00	0.60
$Mg_2Ni^{(20\%)}$ H_4	1.0	6300	300	20.78	0.01	4.76	70.39	1.84	1.74	0.08	0.83
			320	11.00	0.00	2.86	82.90	1.73	1.11	0.05	0.83
			340	8.51	0.01	2.38	86.39	1.86	0.49	0.01	0.82
			360	10.77	0.00	2.43	84.40	1.85	0.17	0.00	0.82
		15,000	360	12.32	0.01	3.11	81.57	1.86	0.27	0.05	0.72
		28,000	360	16.94	0.01	4.00	75.62	1.56	0.26	0.07	0.60
	1.2	6300	300	28.13	0.01	2.47	65.19	1.78	1.89	0.10	0.84
			320	18.41	0.00	0.70	77.73	1.71	1.04	0.04	0.83
			340	16.44	0.00	0.35	80.48	1.76	0.50	0.10	0.82
			360	17.70	0.00	0.22	79.92	1.76	0.02	0.01	0.82
		15,000	360	18.48	0.00	0.63	78.04	1.70	0.24	0.04	0.71

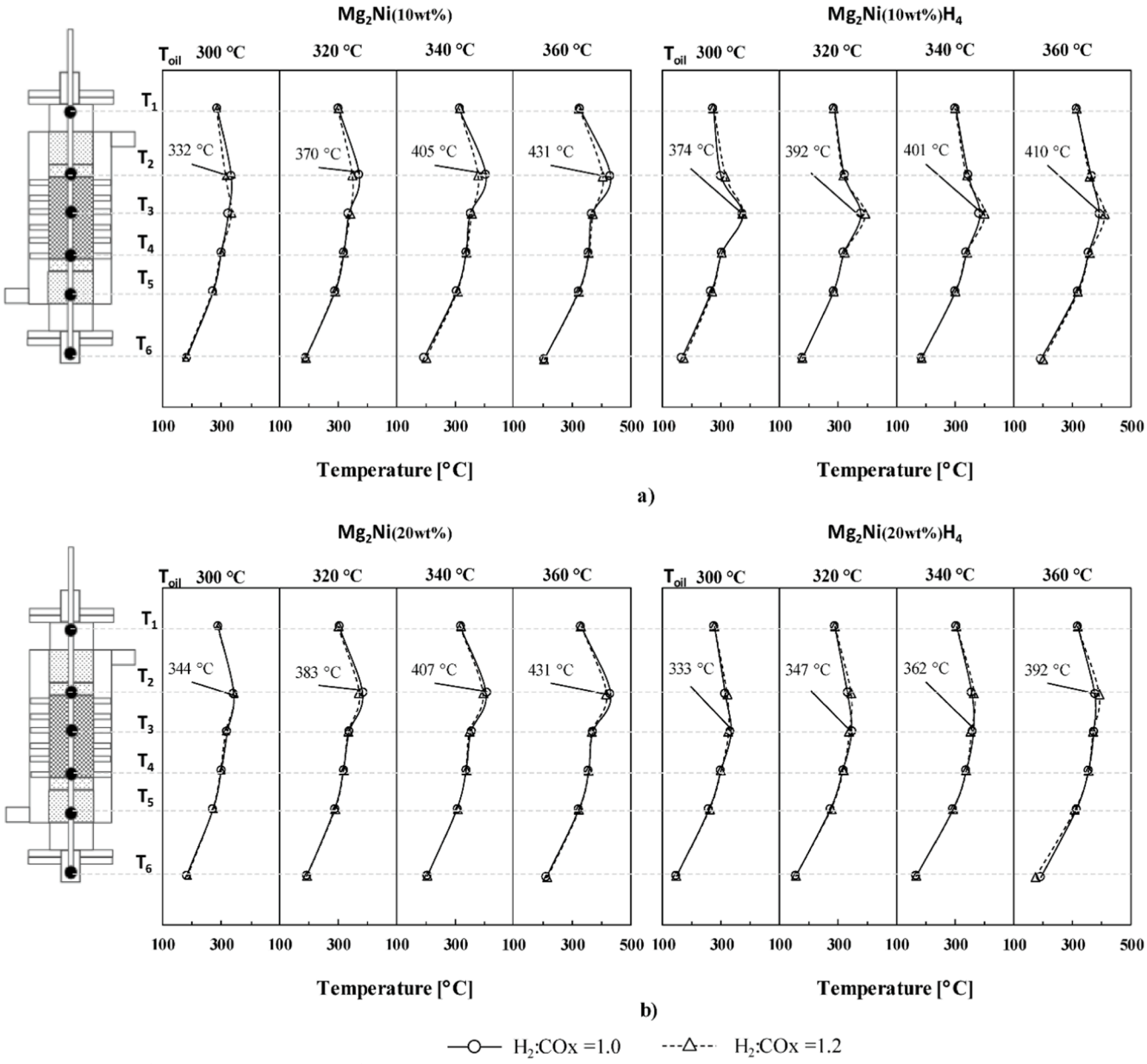

Fig. 7. Reaction temperature profiles for syngas hydrogenation over Mg_2Ni and Mg_2NiH_4 catalyst containing different Ni amount of 10 wt% (a) and 20 wt% (b) at diferent T_{oil}, H_2:CO_x ratios and constant GHSV = 6300 h^{-1}.

associated with the most intense conversion location, i.e. the highest reaction rate, thus leading to an increase in the local temperature. The highest temperature of 431 °C was obtained in point T2 using Mg_2Ni(10 wt%) and Mg_2Ni(20 wt%) catalysts at a thermal oil temperature of 360 °C. Trying to avoid this hot spot, the lower temperature of thermal oil can be used. However, this directly influences conversion efficiency (see the previous section).. The peak temperature point shifts downwards using the Mg_2Ni(10 wt%)H_4 catalyst and is determined at the measurement point T3. However, for all T_{oil}, it was lower than that in Mg_2Ni cases and is related to conversion efficiency (Fig. 4). Most uniform temperature distribution over the height of the reactor was established using the hydrid catalyst with 20 wt% of Ni. The highest temperature was only 392 °C, though it showed the best performance for converting of COx gases. Finally, the products left the catalyst bed with the same temperature as the hot oil (T4) and were further cooled down in the condenser to room temperature.

An increase in the reactant flows through the reactor leading GHSV close to 28000 h^{-1}, results in more marked hot spots. From Fig. 8 can be seen that the maximum temperature shifts down to the thermocouple T3 location and increases up to 466 °C for the Mg_2Ni(10 wt%) alloy and, even more, to 652 °C for the Mg_2Ni(10 wt%)H_4 case. The difference here may be due to catalyst activity. In the case of Mg_2Ni, the reaction seems more widespread over the whole volume as the temperature increase is observed at all points. However, in the case of hydride, there is a slight delay in the onset of the reaction, and once it has occurred, it is more concentrated at one point, which leads to an increase in the temperature. This indicates that the hydrogenated catalyst is more active than the original alloy. The higher Ni content in the catalyst bed reduces the hot spots in the hydride case, and the temperature drops to 515 °C at the maximum GHSV. While the opposite effect is observed with the Mg_2Ni catalyst, where the temperature rises, but not as significantly as in the hydride case Fig. 8.

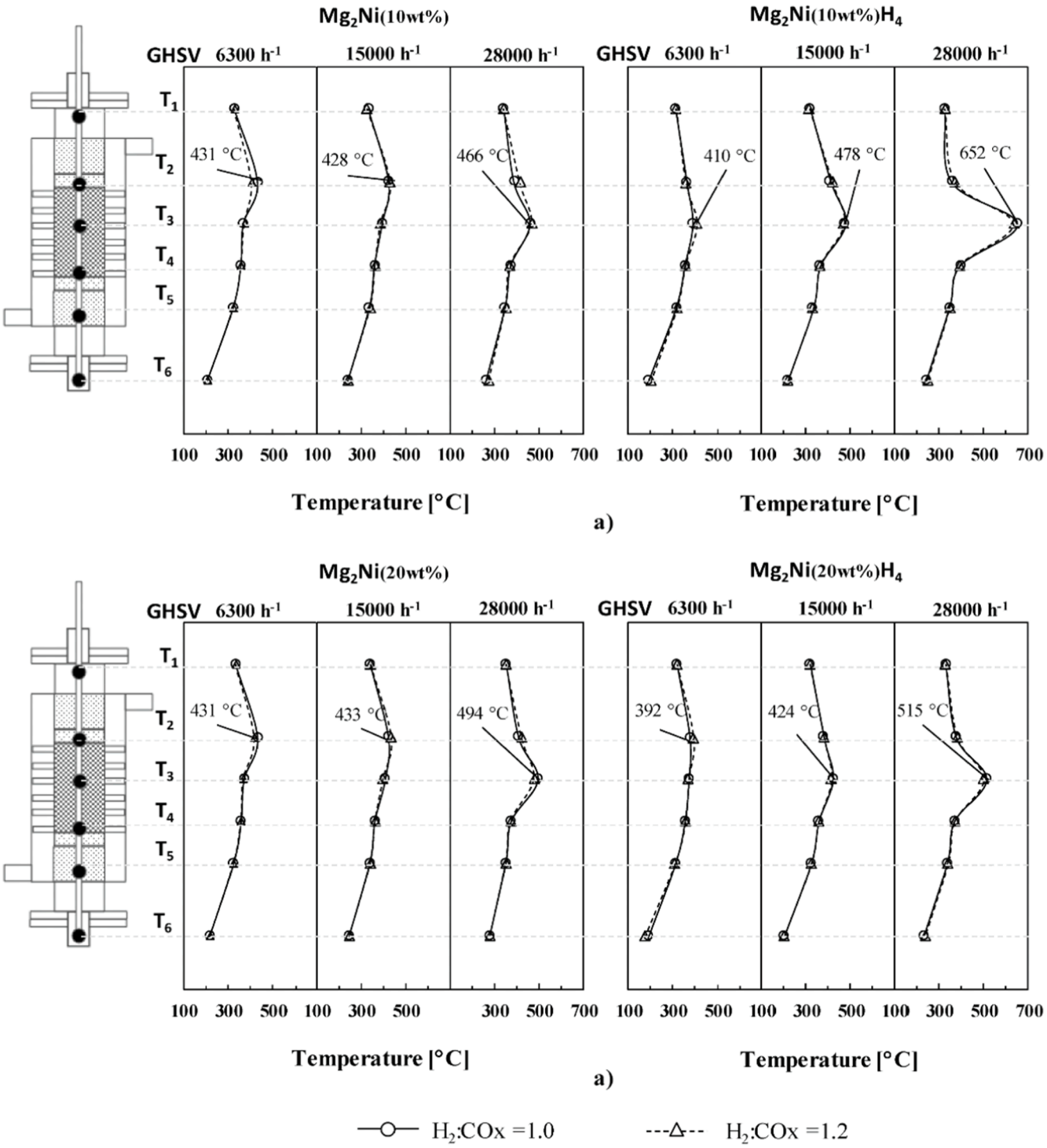

Fig. 8. Reaction temperature profiles for syngas hydrogenation over Mg_2Ni and Mg_2NiH_4 catalyst containing different Ni amount of 10 wt% (a) and 20 wt% (b) at diferent GHSV, H_2:CO_x ratios and constant T_{oil} = 360 °C.

3.3. The energy-mass balance of the optimized biomethane production process chain

The experimental study has identified the optimum conditions for methane synthesis from biomass and its wastes by plasma-assisted gasification. This allows for assessing all the interconnected parts of the process chain and reveals the material and energy needs for developing a preliminary technological concept. The process chain, in this case, is quite simple. First, it consists of the plasma-assisted biomass gasification unit equipped with a gas cleaning system (Fig. 1) capable to generate syngas with suitable characteristics (Table 1). Further, as this study has shown, to achieve complete conversion of COx gas, the hydrogenation process requires additional hydrogen, which could be generated by electrolysis using renewable electricity. The generated syngas and hydrogen thus are fed to the methanation reactor where the conversion, as described in previous sections, takes place. The methanation reactor must have all the necessary equipment, as shown in Fig. 2. After the hydrogenation process, the reaction products get into the condenser, where they are cooled down to room temperature and are separated into water and a mixture of gases comprising mainly of CH_4

(86.4 vol%), unreacted H_2 (8.5 vol%) and CO_2 (2.4 vol%), nitrogen (1.9 vol%) and other trace hydrocarbons (0.8 vol%). Finally, if the methane concentrationhave to be increased from the optimal one obtained in this study, separation of CO_2 and N_2 using polymeric membranes can be installed.

According to the above assumptions, the mass and energy balances for the whole process chain to generate 1MWh of bio-CH_4 were calculated, and results are presented in the Sankey diagrams (Figs. 9 and 10). As can be seen from the mass balance, to produce 1 kg/h of the methane from the proposed technology, the specific material needs would be as follows: 1.16 kg/h of solid and liquid biomass; 1.18 kg/h of steam needed for plasma torch generation and 0.26 kg/h of hydrogen. After the reaction, 1.64 kg/h of the water is formed as a side product after a certain treatment and can be recirculated to generate the steam needed for plasma-assisted gasification. Finally, if the process uses the methane separation unit, a combustible tail gas is also produced, which can be used for heat production and consumed on-site for ongoing processes.

Regarding the energy balance provided in Fig. 10, it can be seen that to generate 1 MWh of bio-CH_4 from biomass using the gasification technology, there is still a need for more than half of the energy in the form of hydrogen, which has to be generated using other means. It is also evident from this diagram that part of the process heat needs can be covered by recovering energy from the water formed in the methanation reaction and used for cooling in the plasmatron. Moreover, waste heat is still available from the cooling of the methanation reactor, which can be further utilised by performing process optimisation.

3.4. *Economic evaluation of the optimized biomethane production process chain*

The production of synthetic bio-methane by gasifying biomass or other wastes is not widely used commercially today. Considering the presented concept of biomethane production from syngas and the obtained results revealing the high conversion, evaluating of the investment required for bio-CH_4 process equipment, commissioning and plant construction was performed for a possible pilot project. For the concept to be developed, a preliminary assessment of the required investment and techno-economic data was carried out based on the “GoBiGas” biomethane plant already in operation [28]. The investments needed for individual technological units and techno-economic data were recalculated for the analysed bio-methane yield of 1 MW. This section provides insights on possible investments estimated under two scenarios: (*bioCH$_4$-case1*) investment for process plants and their commissioning, with a suitable building and infrastructure already in place; (*bioCH$_4$-case2*) greenfield investment. The simulated bio-methane production plant has an output of 1 MWh or an annual output of 8000 MWh/year, assuming an operating time of 8000 h/year. The material and energy balance of the whole process chain to produce 1 MWh of methane output are presented in the previous section and Figs. 9 and 10.

Since countries use different support schemes or types of subsidies to initiate/ encourage the development of innovative technologies, thus it is complicated to evaluate the support or subsidy in a general case, and it is not included in this analysis. Generally, this evaluation targets to provide an economic analysis of the bio-methane plant. It compares the cost of biomethane production with the price of natural gas without taxes under different energy price scenarios:

- high energy price scenario - the price of natural gas (NG) starts at 250€/MWh then annually decreases by 3% from 2023; the biomass price is set to high, 39 €/MWh; high electricity price of 230 €/MWh; the discount rate of 10%;
- medium energy price scenario – the NG price starts at 150€/MWh then annually decrease by 3% from 2023; the biomass price is set to high, 30 €/MWh; high electricity price of 90 €/MWh; the discount rate of 10%;
- low energy price scenario – the NG price starts at 50€/MWh then decrease by 3% annually from 2023; the biomass price is set to high, 15 €/MWh; high electricity price of 30 €/MWh; the discount rate of 10%;
- optimal energy price scenario – the NG price is high, 250 €/MWh; the biomass price is low, 15 €/MWh; the electricity price is medium, 30 €/MWh and the discount rate of 5%.

The factors determining the cost structure of production are the cost of biomass, the cost of energy resources used, and the cost of running facilities. The water demand for the hydrogen production, which is assumed to be 20 l of water per 1 kg of hydrogen [29], was included in the estimation. It is foreseen that the annual water demand will be up to

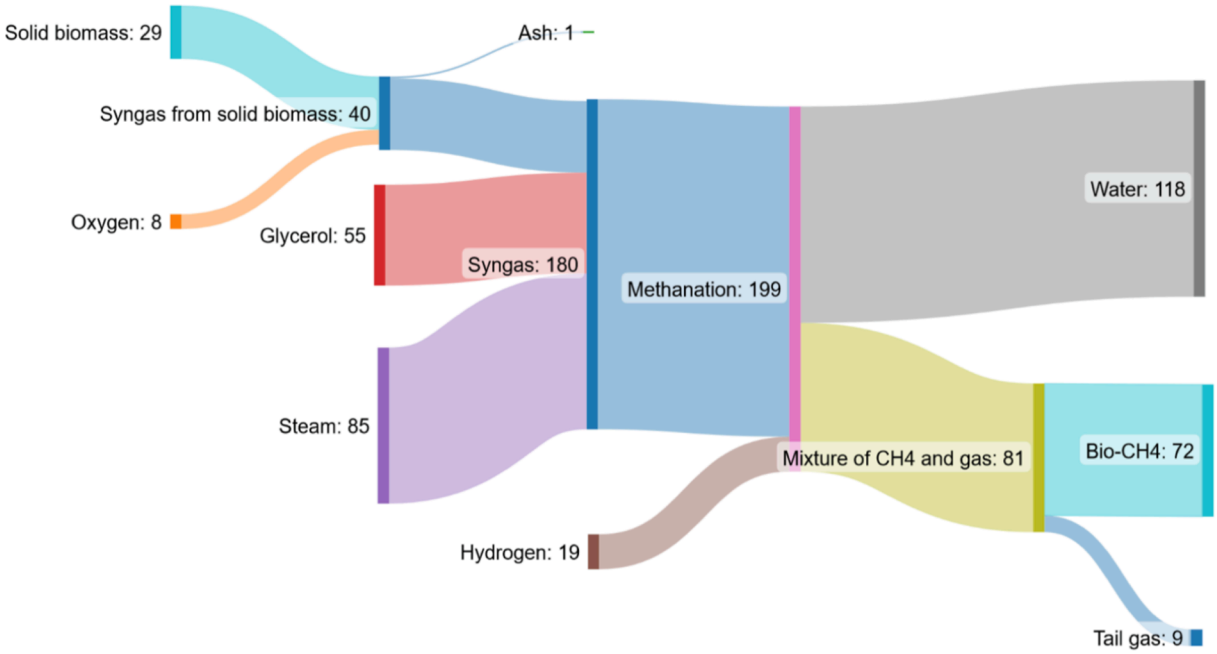

Fig. 9. Sankey diagram of the mass balance (kg/h) of the methanation plant producing 1 MWh of bio-CH_4.

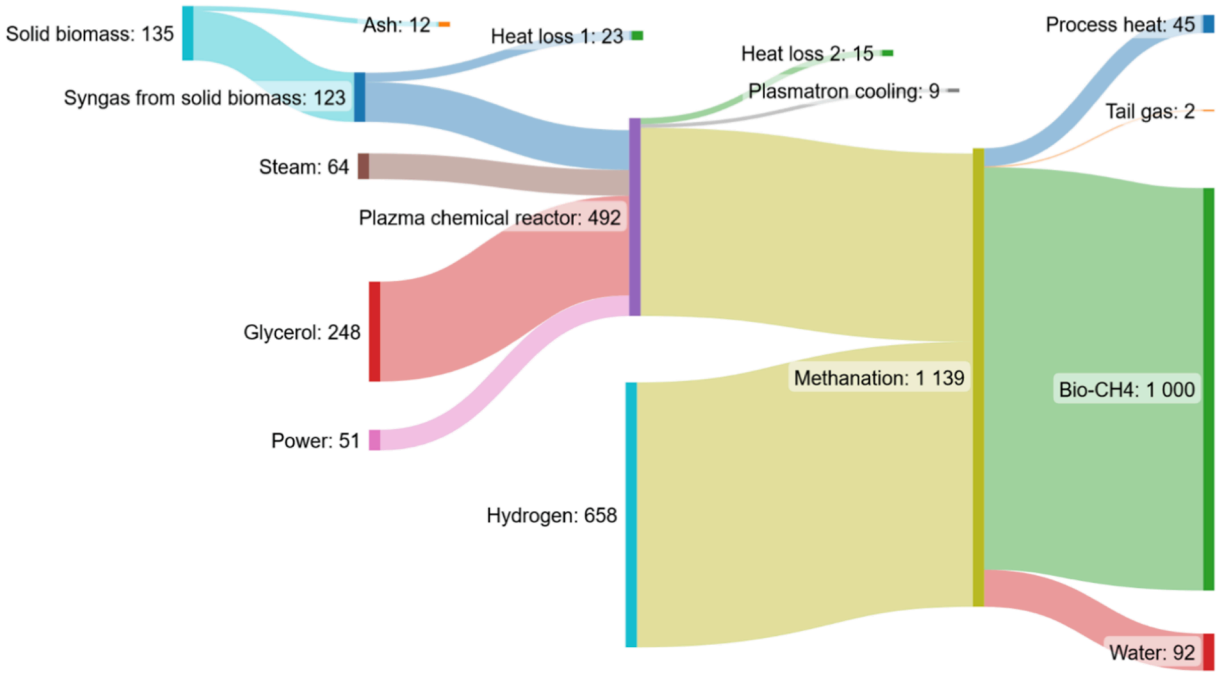

Fig. 10. Sankey diagram of the energy balance (kWh) of the methanation plant producing 1 MWh of bio-CH_4.

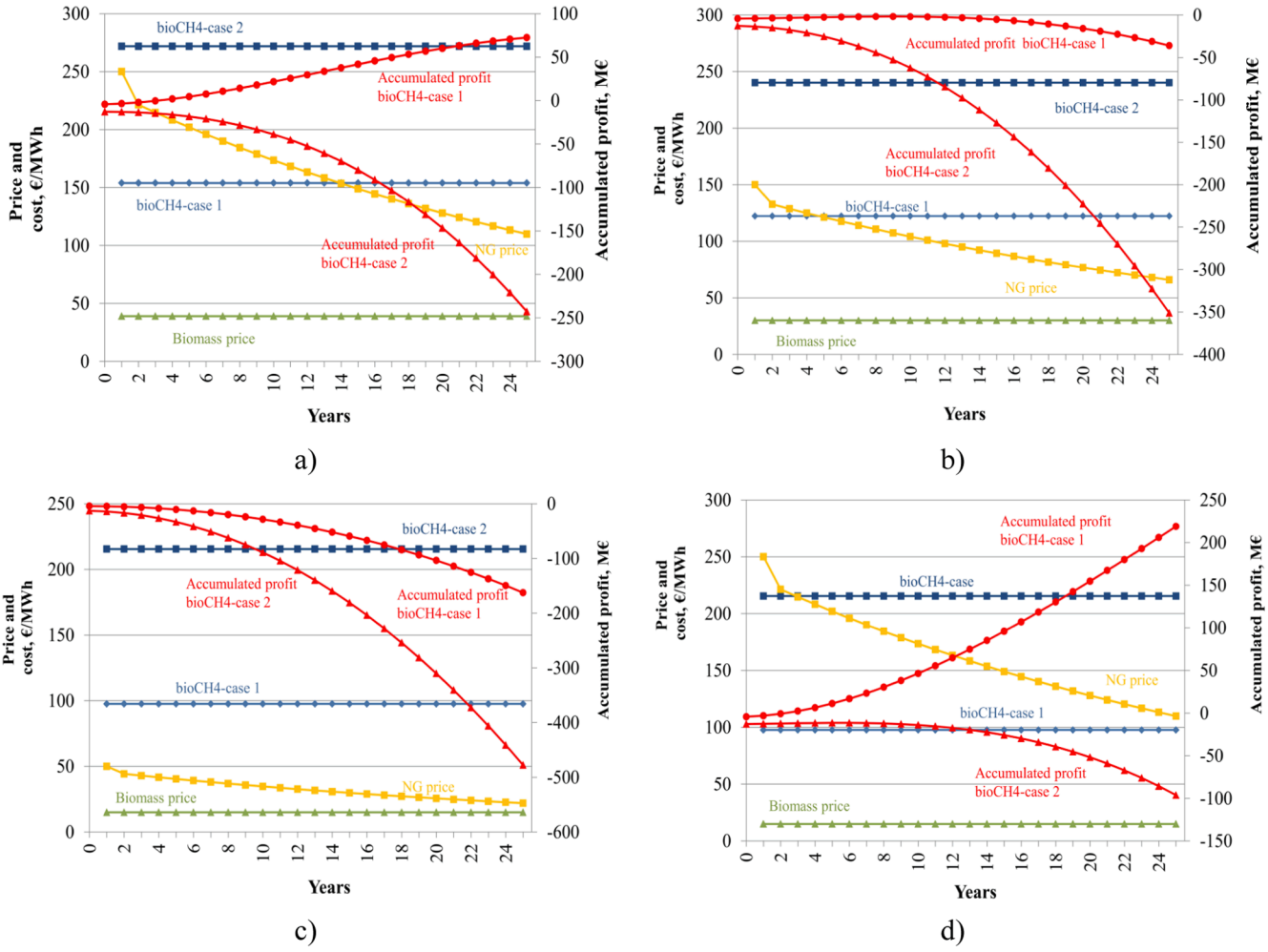

Fig. 11. Bio-methane production costs and accumulated profits for plant (bioCH_4-case1) and greenfield (bioCH_4-case1) investments at different energy price scenarios: a) high; b) medium; c) low; d) optimal.

3000 m^3, and the cost of purchasing and pretreatment water will be up to 8000 €/year. In the highest price scenario, production costs are estimated at 770.8 k€/year with a water component of 1.04 % only; in the medium price scenario, costs are estimated at 517.7 k€/year with a water component of 1.55% only; in the low price scenario, costs are calculated at 320 k€/year with a water component of 2.51% only, and in the optimum price scenario costs are estimated at 397.7 k€/year with a water component of 2.02% only of the total cost of bio-methane production.

The economic evaluation results (Fig. 11) reveal that at both medium and low energy price scenarios, the cost per 1MWh bio-methane production is higher than that of possible natural gas making the production unprofitable. The technology profitability starts when the natural gas prices.

become very high and reach 250 €/MWh. From the provided data, the accumulated profit has already become positive after 4 years of exploitation for the the bioCH_4-case1 at the high price scenario (Fig. 11 a). However, if the technology is necessary to start from the greenfield investments (bioCH_4-case2), the accumulated profit always goes down in any reviewed scenarios. This is related to a high price on the investment of the land, buildings and other necessary infrastructure. It could be pointed out that such units should be installed in the existing energy generation plants, as an example biomass CHP or waste incineration plants, where the necessary infrastructure already exists. Integrating biomethane production, a new plant operation mode based on trigeneration, namely heat, electricity and biofuel in the form of methane, might be initiated.

4. Discussions

This work uses a novel metal hydride catalyst to demonstrate a bio-CH_4 production concept based on plasma gasification and syngas conversion to biomethane. Several key results could be highlighted. Firstly, plasma-assisted gasification generates of a more H_2-enriched gas and an increases in the ratio of the main components needed for the methanation reaction. This reduces the need for hydrogen, essential for high conversion efficiency. As seen from Sankey's energy flow diagram (Fig. 10), even though the H_2 content of the gas is increased, the energy contribution of the additional hydrogen makes up most of the energy input to methane production. On the one hand, this is not a bad thing, especially when the installation capacity of renewable energy sources (wind and solar) is currently being increased and, in the event of a surplus of electricity on the market, hydrogen could be produced through electrolysis and stored as chemical energy in the form of methane.

A second key result would be using of a new type of catalyst. As already mentioned in the introduction, it is known that the synergy of bimetallic composites enhances the performance of catalysts at lower temperatures while remaining active for longer periods [15]. Our experiments have shown that this type of catalyst achieves very high COx gas conversion and high methane concentration in the gaseous products. In addition, the by-products of the reaction at the best case are also not high, e.g. H_2 residue 8.51 vol%, CO_2 – 2.38 vol%, CO less than 0.01 vol %, N_2 – 1.86 vol%, other light C_nH_m less than 0.5 vol%. A gas of this composition could be fed directly into the natural gas network without significantly altering the existing infrastructure.

The third outcome relates to the commercialisation of the technology and the limits that arise with the technology's payback. As the economic analysis of the technology has shown, the attractiveness of the technology only comes into play when the price of natural gas on the market is extremely high, reaching up to 250 €/MWh, even though the cost of raw materials and electricity would be low. As the final technology was not developed at the time of this study, it would not have been easy to estimate the realistic CAPEX and OPEX. Thus the payback period assessment was done according to costs found in the literature [27,28] while applying a scaling factor for the selected capacity. This methodology may introduce some deviation, but that would not be the limiting factor for the profitability evaluation. Further studies on catalyst long-term activities could assess whether a simplified syngas cleaning technology such as that used in this work would be feasible. Such simplification would certainly allow a reduction in CAPEX and thus be more competitive with existing fossil energy sources. Also, further policy decisions to move towards higher RES integration and higher CO_2 emission taxes would further contribute to increasing the competitiveness and development of the technology.

5. Conclusions

After conducting an experimental validation study of technology based on integrated plasma-assisted biomass gasification to biomethane production, it was established:

The synergism of the two-metal Mg and Ni alloy for the catalytic selectivity of COx gas and conversion to CH_4 was determined. The highest COx in syngas conversion $X_{COx} = 0.997$ was determined using $Mg_2Ni(_{20\ wt\%})H_4$ at an H_2:COx ratio of 1.2, reactor temperature of 360 °C and GHSV of 6300 h^{-1}. The methane concentration at this point was $Y_{CH4} = 79.9$ vol%. Aiming to get higher content of methane ($Y_{CH4} =$ 86.4 vol%) in gas, the process parameter should be optimised as follows - catalyst $Mg_2Ni(_{20\ wt\%})H_4$, H_2:COx ratio of 1.0, reactor temperature of 360 °C and GHSV of 6300 h^{-1}, which makes a bit lower conversion ($X_{COx} = 0.968$) and process efficiency.

The non-hydrogenated (Mg_2Ni) catalyst activity for COx gas conversion and CH_4 production showed similar results in the hydride catalyst case. The higher activity of the Mg_2NiH_4 catalyst in the change of GHSV was obtained. The latter also showed much more sensitivity to the reactor temperature changes than the non-hydrogenated one and was more effective at a lower process temperature. It was also established that in the case of a hydrogenated metal, due to released hydrogen, the methanation reaction (process) starts faster than using a non-hydrogenated metal alloy.

The preliminary economic evaluation showed that the technology profitability starts when the natural gas prices are very high and reach 250 €/MWh. In such a case, the accumulated profit becomes positive already after 4 years of exploitation. However, if the technology is necessary to start from the greenfield investments, the accumulated profit is always negative. Therefore, this study revealed that biomethane production should be installed in the existing energy generation plants to initiate a new, more flexible plant operation mode based on the trigeneration, namely heat, electricity and biofuel in the form of methane.

CRediT authorship contribution statement

Nerijus Striūgas: Conceptualization, Methodology, Supervision, Writing – original draft, Writing – review & editing. **Kęstutis Zakarauskas:** Data curation, Investigation, Resources, Writing – review & editing. **Rolandas Paulauskas:** Visualization, Formal analysis, Writing – original draft. **Aurimas Lisauskas:** Software, Validation, Writing – original draft. **Adolfas Jančauskas:** Writing – original draft, Writing – review & editing.

Declaration of Competing Interest

The authors declare that they have no known competing financial interests or personal relationships that could have appeared to influence the work reported in this paper.

Data availability

Data will be made available on request.

Acknowledgment

The research was funded by the European Regional Development Fund according to the supported activity "Research Projects Implemented by World-class Researcher Groups" under Measure No. 01.2.2-LMT-K-718 (grant No. 01.2.2-LMT-K-718-01-0005) from the Research Council of Lithuania. Special thanks goes to the rest project team members: Martynas Lelis, Andrius Tamošiūnas, Vilma Snapkauskienė.

References

[1] Eisavi B, Ranjbar F, Nami H, Chitsaz A. Low-carbon biomass-fueled integrated system for power, methane and methanol production. Energy Convers Manag 2022;253:115163. https://doi.org/10.1016/j.enconman.2021.115163.
[2] Puricelli S, Cardellini G, Casadei S, Faedo D, van den Oever AEM, Grosso M. A review on biofuels for light-duty vehicles in Europe. Renew Sustain Energy Rev 2021;137:110398. https://doi.org/10.1016/j.rser.2020.110398.
[3] Menin L, Asimakopoulos K, Sukumara S, Rasmussen NBK, Patuzzi F, Baratieri M, et al. Competitiveness of syngas biomethanation integrated with carbon capture and storage, power-to-gas and biomethane liquefaction services: techno-economic modeling of process scenarios and evaluation of subsidization requirements. Biomass Bioenergy 2022;161:106475. https://doi.org/10.1016/j.biombioe.2022.106475.
[4] Sikarwar VS, Zhao M, Fennell PS, Shah N, Anthony EJ. Progress in biofuel production from gasification. Prog Energy Combust Sci 2017;61:189–248. https://doi.org/10.1016/j.pecs.2017.04.001.
[5] Arregi A, Amutio M, Lopez G, Bilbao J, Olazar M. Evaluation of thermochemical routes for hydrogen production from biomass: a review. Energy Convers Manag 2018;165:696–719. https://doi.org/10.1016/j.enconman.2018.03.089.
[6] Giglio E, Vitale G, Lanzini A, Santarelli M. Integration between biomass gasification and high-temperature electrolysis for synthetic methane production. Biomass Bioenergy 2021;148:106017. https://doi.org/10.1016/j.biombioe.2021.106017.
[7] Hlina M, Hrabovsky M, Kavka T, Konrad M. Production of high quality syngas from argon/water plasma gasification of biomass and waste. Waste Manag 2014;34:63–6. https://doi.org/10.1016/j.wasman.2013.09.018.
[8] Centi G, Perathoner S. Opportunities and prospects in the chemical recycling of carbon dioxide to fuels. Catal Today 2009;148:191–205. https://doi.org/10.1016/j.cattod.2009.07.075.
[9] Materazzi M, Lettieri P, Mazzei L, Taylor R, Chapman C. Reforming of tars and organic sulphur compounds in a plasma-assisted process for waste gasification. Fuel Process Technol 2015;137:259–68. https://doi.org/10.1016/j.fuproc.2015.03.007.
[10] Yoon SJ, Yun YM, Seo MW, Kim YK, Ra HW, Lee J-G. Hydrogen and syngas production from glycerol through microwave plasma gasification. Int J Hydrogen Energy 2013;38:14559–67. https://doi.org/10.1016/j.ijhydene.2013.09.001.
[11] Tamošiūnas A, Gimžauskaitė D, Aikas M, Uscila R, Zakarauskas K. Waste glycerol gasification to syngas in pure DC water vapor arc plasma. Int J Hydrogen Energy 2022;47:12219–30. https://doi.org/10.1016/j.ijhydene.2021.06.203.
[12] Saeidi S, Najari S, Hessel V, Wilson K, Keil FJ, Concepción P, et al. Recent advances in CO2 hydrogenation to value-added products — current challenges and future directions. Prog Energy Combust Sci 2021;85:100905. https://doi.org/10.1016/j.pecs.2021.100905.
[13] Liu H, Zou X, Wang X, Lu X, Ding W. Effect of CeO2 addition on Ni/Al2O3 catalysts for methanation of carbon dioxide with hydrogen. J Nat Gas Chem 2012;21:703–7. https://doi.org/10.1016/S1003-9953(11)60422-2.
[14] Pieta IS, Lewalska-Graczyk A, Kowalik P, Antoniak-Jurak K, Krysa M, Sroka-Bartnicka A, et al. CO2 hydrogenation to methane over Ni-catalysts: the effect of support and vanadia promoting. Catalysts 2021;11:433. https://doi.org/10.3390/catal11040433.
[15] Lv C, Xu L, Chen M, Cui Y, Wen X, Li Y, et al. Recent progresses in constructing the highly efficient Ni based catalysts with advanced low-temperature activity toward CO2 methanation. Front Chem 2020;8:1–32. https://doi.org/10.3389/fchem.2020.00269.
[16] Li Y, Lu G, Ma J. Highly active and stable nano NiO-MgO catalyst encapsulated by silica with a core-shell structure for CO2 methanation. RSC Adv 2014;4:17420–8. https://doi.org/10.1039/c3ra46569a.
[17] Feng X, Feng J, Li W. Insight into MgO promoter with low concentration for the carbon-deposition resistance of Ni-based catalysts in the CO2 reforming of CH4. Cuihua Xuebao/Chinese J Catal 2018;39:88–98. https://doi.org/10.1016/S1872-2067(17)62928-0.
[18] Yan Y, Dai Y, He H, Yu Y, Yang Y. A novel W-doped Ni-Mg mixed oxide catalyst for CO2 methanation. Appl Catal B Environ 2016;196:108–16. https://doi.org/10.1016/j.apcatb.2016.05.016.
[19] Loder A, Siebenhofer M, Lux S. The reaction kinetics of CO2 methanation on a bifunctional Ni/MgO catalyst. J Ind Eng Chem 2020;85:196–207. https://doi.org/10.1016/j.jiec.2020.02.001.
[20] Liu J, Cui D, Yu J, Su F, Xu G. Performance characteristics of fluidized bed syngas methanation over Ni–Mg/Al2O3 catalyst. Chinese J Chem Eng 2015;23:86–92. https://doi.org/10.1016/j.cjche.2014.09.038.
[21] Wang T, Chang J, Cui X, Qi Zhang YF. Reforming of raw fuel gas from biomass gasification to syngas over highly stable nickel–magnesium solid solution catalystse. Fuel Process Technol 2006;87:421–8.
[22] Bartik A, Fuchs J, Pacholik G, Föttinger K, Hofbauer H, Müller S, et al. Experimental investigation on the methanation of hydrogen-rich syngas in a bubbling fluidized bed reactor utilizing an optimized catalyst. Fuel Process Technol 2022:237. https://doi.org/10.1016/j.fuproc.2022.107402.
[23] Kato S, Borgschulte A, Ferri D, Bielmann M, Crivello JC, Wiedenmann D, et al. CO 2 hydrogenation on a metal hydride surface. Phys Chem Chem Phys 2012;14:5518–26. https://doi.org/10.1039/c2cp23264b.
[24] Lelis M, Varnagiris S, Urbonavicius M, Zakarauskas K. Investigation of catalyst development from Mg2NiH4 hydride and its application for the CO2 methanation reaction. Coatings 2020;10:1178. https://doi.org/10.3390/coatings10121178.
[25] Striugas N, Zakarauskas K, Džiugys A, Navakas R, Paulauskas R. An evaluation of performance of automatically operated multi-fuel downdraft gasifier for energy production. Appl Therm Eng 2014;73:1151–9. https://doi.org/10.1016/j.applthermaleng.2014.09.007.
[26] Su X, Xu J, Liang B, Duan H, Hou B, Huang Y. Catalytic carbon dioxide hydrogenation to methane: a review of recent studies. J Energy Chem 2016;25:553–65. https://doi.org/10.1016/j.jechem.2016.03.009.
[27] Holmgren KM. NUMBER B 2221 Investment cost estimates for gasification- based biofuel production systems. Stockholm; 2015.
[28] Thunman H, Gustavsson C, Larsson A, Gunnarsson I, Tengberg F. Economic assessment of advanced biofuel production via gasification using cost data from the GoBiGas plant. Energy Sci Eng 2019;7:217–29. https://doi.org/10.1002/ese3.271.
[29] Simoes SG, Catarino J, Picado A, Lopes TF, di Berardino S, Amorim F, et al. Water availability and water usage solutions for electrolysis in hydrogen production. J Clean Prod 2021;315:128124. https://doi.org/10.1016/j.jclepro.2021.128124.